

| | | | |
|---|---|-------------------------------|--|
|  | SAKARYA UNIVERSITY JOURNAL OF SCIENCE | |  SAKARYA UNIVERSITY |
| | e-ISSN: 2147-835X | | |
| | http://www.saujs.sakarya.edu.tr | | |
| Recieved 2018-02-24 | Accepted 2018-06-22 | DOI 10.16984/saufenbilder. | |

Numerical investigation for convection heat transfer and friction factor under pulsatile flow conditions

Erman Aslan^{*1}

ABSTRACT

Numerical investigation is made for understanding convection heat transfer and friction factor characteristic under pulsatile flow conditions at the periodic wavy channels. In the numerical study, the Finite Volume Method (FVM) is used. Reynolds Averaged Numerical Simulations (RANS) based turbulence models which are the $k-\omega$, the Shear Stress Transport (SST) and the transition SST, are employed and compared each other. The results are also compared with the previous measurements performed for non-pulsating conditions. Air flow through wavy channel, which has sharp corrugation peak with an inclination angle of 30° and 5mm minimum channel height, is done. Reynolds number is taken from 6294 to 7380, and Prandtl number is kept 0.7. Four different sinusoidal pulsatile flow conditions, which are combination of two different frequencies and two different amplitudes, are used. Amplitude and period of pulsatile flow effects are discussed

Keywords: Wavy Channel, Convection Heat Transfer, Friction Factor, Finite Volume Method, RANS based Turbulence Models, Pulsatile Flow Conditions

1. INTRODUCTION

Lately, requirement of more efficient and compact exchanges is increased, therefore, exploration heat transfer augmentation methods has attained great momentum. On account of this purpose, two techniques can be specified which names are the active and passive techniques [1]. Active techniques contains surface and fluid vibration, boundary layer injection and suction, electrostatic fields, electro-hydrodynamics to enhance heat transfer. Thus, active techniques require more costs and attention [2].

Generally in passive techniques, channel geometry is modified for increasing heat transfer. Using bluff bodies is one of the special category of heat transfer enhancement in passive techniques. In channels, usage of triangular prism

enhances convection heat transfer coefficients by turbulence generation and vortex shedding in their wake [3, 4]. In a channel, the insertion of structures such a twisted tapes is one of passive techniques. Twisted tapes stimulate a swirling motion, where the swirl components increases velocities and shear stresses near the walls, therefore, convective transport ability of the fluid is increased [5]. Passive methods may also include categoric changes in the flow arrangement, such as the use of jet impingement techniques [6] instead of wall-congruent flow, which is, however, out of the present scope. Increasing of the heat transfer with radiation [7] is not contained in the present scope. The present focus is on the augmentation of heat transfer by forced convection. A combination of passive and active techniques is considered, in the present investigation. The use of wavy channels and

^{*} Corresponding author

¹ Istanbul University, Faculty of Engineering, Mechanical Engineering Dept., Istanbul, Turkey- erman.aslan@istanbul.edu.tr

pulsatile inlet flow conditions belong to the passive and active categories, respectively.

In wavy channels, experimental investigations for understanding heat transfer and friction factor characteristics were studied by Sparrow and Hossfeld [8], Snyder et al. [9], Bilen et al. [10] and Nilpueng and Wongwises [11]. Additionally, in corrugated channel, computational investigation of forced convection in turbulent regimes were performed to get convection heat transfer coefficient and friction factor by Ciafalo et al. [12] and Mirzaei et al. [13].

In many engineering applications and also in nature and biological system, pulsatile flows are encountered. One of the engineering applications is pulsating flow in pipe and channels. In moderate and high Reynolds number regimes, development length is determined under sinusoidal pulsatile laminar pipe flows analytically and numerically by Ray et al [14]. Hydrodynamics of piston-driven laminar pulsating flow for developing flow was studied numerically at $Re=1000$ by Aygun and Aydin [15]. Five different values of the frequencies were considered. They observed that friction factors rises with frequency. In second paper of Aygun and Aydin, piston-driven laminar pulsatile flow hydrodynamics for fully developed flow was investigated numerically, analytically and experimentally [16]. Again five different frequency values were determined like in first paper [15]. Near the walls, flow reversals at $F=105$, 226 and 402, where F is the non-dimensional frequency. In the laminar regime, numerical study for determining velocity and temperature fields in circular tube under pulsatile flow condition is done by Chattopadhyay et al [17]. The frequency interval was taken from 0 to 20Hz, and amplitude was determined to be greater than one. It was observed that, pulsatile flow supports negative effect in increasing heat transfer within investigated range of pulsation amplitude and frequency. In a straight circular tube, a computational investigation of the pulsatile flow and heat transfer for the turbulent flow regime was presented by Benim et al [18]. In this study, it was observed that, there is no significant enhancement of the time-averaged rate of heat

transfer by pulsations for the considered conditions.

In a parallel plates and or a circular tube, in order to obtain analytical expression for the velocity and temperature distribution and unsteady Nusselt number for the forced convection problem, a perturbation approach was used by Nield and Kuznetsov [19]. Pulsatile flow conditions were formed with using pressure gradients. It was observed that, Nusselt number alters with frequency. In another investigation, closed-loop pulsatile heat pipes performance with uniform and altering tube diameter was investigated experimentally by Tseng et al. [20].

In a square mini-channel, Metha and Khandekar was made experimental study in order to determine convection heat transfer of single-phase pulsating laminar flow [21]. According to results, frequency has an important role for convection heat transfer. With increasing frequency, heat transfer rate increases. Yu et al [22] made numerical investigation in order to understand characteristics of flow and heat transfer under pulsatile flow conditions, in a heated square cylinder. In the pulsatile flow, amplitude and frequency were changing in the range 0.2 - 0.8[-] and 0 - 20Hz, respectively. It was found that, if the pulsatile frequency is about natural vortex shedding frequency, convection heat transfer was also highly augmented. Jafari et al [23] investigated convection heat transfer for pulsating flow conditions with using Lattice Boltzmann Method. The dimensionless frequency of pulsating velocity and oscillating amplitude were studied at a wide range (Strouhal number, from 0.05 to 1, and amplitude, from 0 to 0.25, where amplitude is equal to "0" represents the steady flow). Pulsating flows also occur in biological systems, such as the blood flow in human aorta under physiological, or surgery conditions, and have been investigated experimentally and computationally by different researchers [24-27].

In the present study, characteristics of convection heat transfer and friction factor in a wavy channels with pulsatile flow conditions are investigated. In the numerical analysis, the finite volume method is used. Only one type wavy

geometry is used which has sharp corrugation peak. Four different cases are considered in the simulations, which result out of the combination of two different frequencies and two different amplitudes. Three different RANS based turbulence models, which are the $k-\omega$, the Shear Stress Transport (SST) and the transition SST, are used

2. PROBLEM DEFINITION

A symmetrically corrugated channel with sharp corrugation peaks is considered. The schematic of channel with the geometry parameters is shown in Figure 1. Contact angle (θ) is 30° , pitch or axial length of loop (S) is 17.32mm, channel half height (b) is 7.5mm and height of corrugation (a) is 5mm.

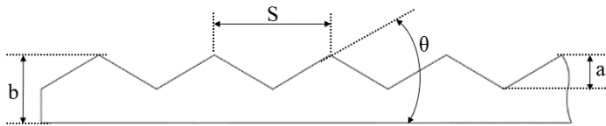


Figure 1. Schematic figure of corrugation channel with the representative parameters

According to these parameters maximum channel height is described as;

$$H_{\max} = 2b \tag{1}$$

the minimum channel height is taken by;

$$H_{\min} = 2(b - a) \tag{2}$$

The hydraulic diameter is defined as;

$$D_h = H_{\min} + H_{\max} \tag{3}$$

Reynolds number (Re) is taken from 6294 to 7380, and Prandtl number is kept 0.70.

In the numerical calculations, two-dimensional assumption is used. Air properties are assumed to be constant. In Figure 2, representative of solution domain with boundary types is shown. A sinusoidal velocity profile in time is applied for getting pulsating flow conditions at the inlet. Sinusoidal velocity profile is defined as;

$$u(t) = u_0 [1 + u_A^* \sin(2\pi ft)] \tag{4}$$

where u_0 is the uniform inlet velocity, f is frequency, t is time and u_A^* is

nondimensionalized amplitude. The nondimensionalized amplitude is defined as;

$$u_A^* = \frac{u_A}{u_0} \tag{5}$$

where u_A is amplitude. Nondimensionalized frequency F is defined as;

$$F = \frac{D_h^2 f}{\nu} \tag{6}$$

where ν is the kinematic viscosity. The Reynolds number is described as

$$Re = \frac{\rho u_0 D_h}{\mu} \tag{7}$$

where ρ and μ are density and dynamic viscosity, respectively. With combining two different nondimensionalized amplitudes (0.25 and 0.5) and two different nondimensionalized frequencies (200 and 400), four different cases are determined, in order to understand effect of frequency and amplitude on Nusselt number and friction factor. Cases are shown in Table 1.

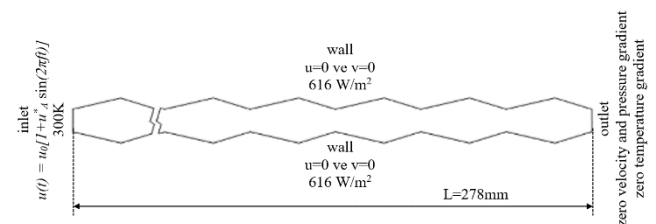


Figure 2. A representative of solution domain with boundary types

Table 1. Cases for pulsating flow

| Case number | F | u_A^* |
|-------------|-----|---------|
| 1 | 200 | 0.25 |
| 2 | 200 | 0.5 |
| 3 | 400 | 0.25 |
| 4 | 400 | 0.5 |

At the outlet, an outflow boundary condition which means zero velocity and pressure gradients is imposed for momentum equations. Additionally, no-slip boundary condition is applied at walls. For the energy equation, constant temperature (300K) is imposed at the inlet. At walls, a constant heat flux (616 W/m^2) is applied. Finally, at the outlet, zero temperature gradient is defined.

3. MODELLING AND ASSUMPTIONS

Time unsteady incompressible Navier-Stokes equations is working together equation of continuity, equation of energy and equations of turbulence models. These equations are discretised by the finite volume based commercial CFD code Ansys-Fluent [28]. Three different RANS based turbulence models are used which are $k-\omega$, [29] SST [30] and transition SST [31]. Wall-functions are no used for these turbulence models [32]. If the grid resolution is fine enough near the walls, turbulence equations can represent the near-walls turbulence.

For discretizing convective terms a second-order upwinding procedure is applied [28]. For time integration, a second-order implicit scheme is used. PISO algorithm is employed in order to couple pressure and velocity. For momentum, energy and turbulence equations, default under-relaxation factors are used. As the converge criteria, two different residual value are used. Firstly, residual value is 10^{-8} is used for only energy equations. The other value is 10^{-6} is applied for all equations except energy equations. Intensity and length scale of turbulence at the inlet is taken 4% and one third of hydraulic diameter, respectively.

Quadrilateral meshes are used. A grid independence study applied in order to find sufficient number of grids for all turbulence models and four cases. Two quantities are taken into account for grid independence study. These quantities are Nusselt number and friction factor. The grid independence study was conducted for steady-state flow conditions. Doing so, the maximum temporal flow rate of the pulsating flow is assumed to be the flow rate in the steady-state. This means that the velocity $u_{\max} = u_0 + u_A$, is prescribed at the inlet, where u_0 is taken from the maximum Reynolds number. Although, external boundary layer which means inflation is not used at walls, for getting laminar-sub layer fine meshes are used at walls. For the first near-wall cell and the at least three cells $y^+ < 1$ and $y^+ < 5$ is ensured, respectively, in order to represent near-wall in all turbulence models. For all turbulence models, and four cases, the grid independence mesh number is 192000. Value of cell Courant number is taken as

one for stability of unsteady calculations. Therefore, for choosing time step size, this stability issue is taken into account. The maximum skewness ratio is 0.150883 and maximum aspect ratio is 8.06939.

Two parameters are taken into account for the present study, which are (1) Nusselt number and (2) friction factor. In numerical calculations, loop averaged Nusselt number is calculated as

$$Nu = \frac{hD_h}{k} \quad (8)$$

where k is the thermal conductivity and h is the loop averaged heat transfer coefficient.

In computational calculations, local heat transfer coefficient (h_x) at the former three loops from the last loop are computed, with using time-averaged wall and fluid temperatures. After that, the loop averaged heat transfer coefficient is obtained via the local heat transfer coefficients.

$$h = \frac{1}{3S} \int_0^{3S} h_x dx \quad (9)$$

In numerical simulations, two sections are specified to determine the pressure gradient (dP/dx). The first section and second sections are placed at the beginning of the former three loops from the last loop and on the end of the previous loop from the last loop, respectively.

With using pressure gradients, friction factor is determined.

$$f = -\frac{dP}{dx} D_h \left/ \frac{1}{2} \rho u_0^2 \right. \quad (10)$$

4. RESULTS AND DISCUSSIONS

The predictions of the time-averaged axial velocity distribution function is shown at Figure 3. Figure 3(a), Figure 3(b) and Figure 3(b) presents the predictions of $k-\omega$, SST and transition SST turbulence models, respectively. These distributions are obtained for the highest Reynolds number ($Re=7380$). The flow develops through the wavy channels. Flow characteristics are not changed at the last loops of the wavy channels. Therefore, we can observe periodicity or fully-developed regime. The

periodicity is observed for all three turbulence models. The flow is reached the fully-developed regime earlier at the lower Reynolds number, which is not presented here. The predictions of three turbulence models almost almost the same.

The computed time-averaged temperature distribution by (a) $k-\omega$, (b) SST and (c) transition SST turbulence model is shown in Figure 4 for the highest Reynolds number ($Re=7380$). Because of using constant heat flux at the wavy walls, temperature of flow is arised leisurely and continually. At the boundaries, flow is recirculated because wavy forms, therefore temperature gradients at the normal of the wavy walls are also observed. These temperature gradients supports to become heat transfer. The $k-\omega$ turbulence model produce higher temperature is than the other turbulence models.

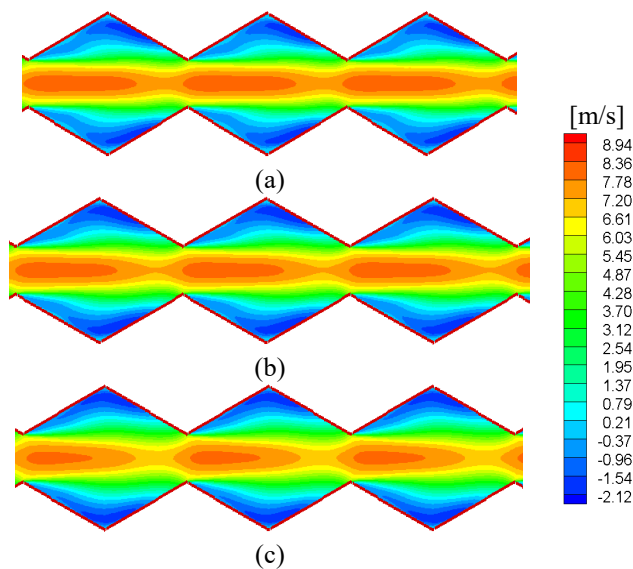


Figure3. Time-averaged axial velocity contours for (a) $k-\omega$, (b) SST, (c) transition SST

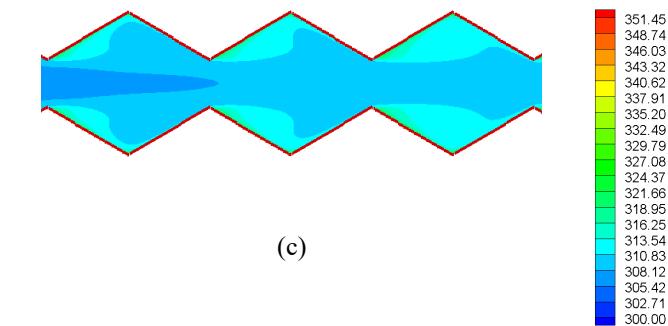
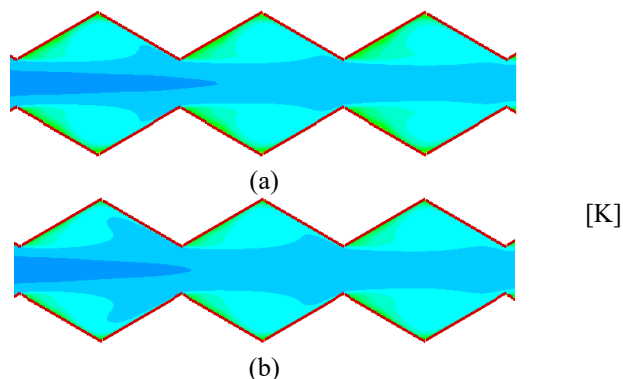


Figure 4. Time-averaged temperature contours for (a) $k-\omega$, (b) SST, (c) transition SST

Figure 5 presents the changing of Nusselts numbers with Reynolds number for (Figure 5a) $k-\omega$, (Figure 5b) SST and (Figure 5c) transition SST turbulence models. The curves for the four considered cases and the experimental results for the non-pulsating flow conditions [33] are presented and compared with each other in Figure 5. One can see that, Nusselt number decreases with decreasing Reynolds numbers for all cases, as predicted by all turbulence models. Case-4 produces the largest Nusselt number value for all turbulence models, This is followed by Case-2, and then by Case-1 and Case-3, in the order of decreasing Nusselt number. Amplitude has a positive effect on the Nusselt number. In SST and transition SST turbulence models, the experimental, steady-state Nusselt number is lower than for pulsating cases. In a previous study [33], the SST turbulence model was found to perform better than the other turbulence modes. A superior performance of the SST model in predicting convective heat transfer was also observed by other authors [34,35]. Based on these findings, and, thus, assuming that the SST turbulence model is sufficiently accurate, we can conclude that pulsating flow conditions has a positive effect for enhancing heat transfer. However, non-pulsating experimental results is larger than the pulsating numerical results for the $k-\omega$ turbulence model. In order to clarify this conflict, experiments need to be made with pulsating flow conditions.

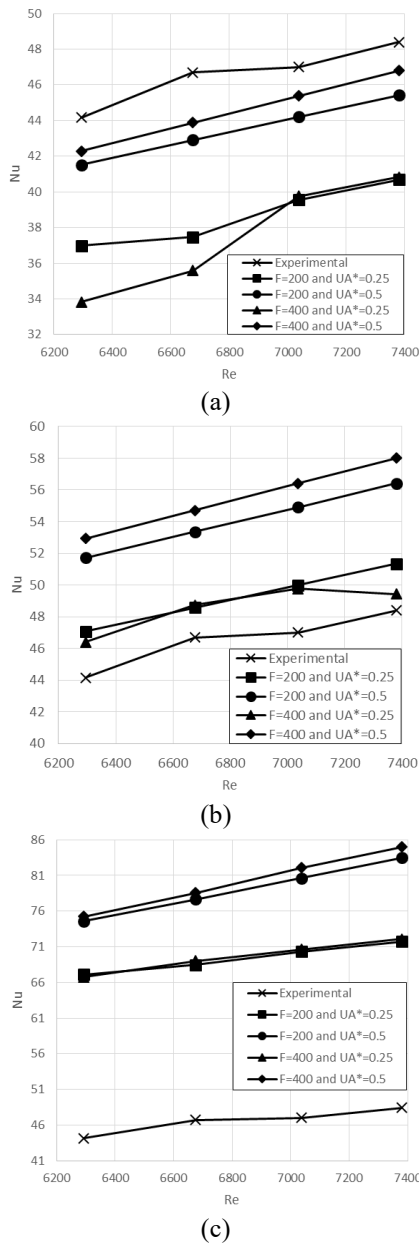


Figure 5. Changing of Nusselt numbers with Reynolds numbers for (a) $k-\omega$ (b) SST (c) transition SST turbulence models

The changing of friction factors with Reynolds number is shown for $k-\omega$ (Figure 6a), SST (Figure 6b) and transition SST (Figure 6c) in Figure 6. Again, the curves for the four considered cases and the experimental results for the non-pulsating conditions [33] are presented and compared each other in Figure 6. One can see that, the friction factors decreases with Reynolds numbers except for the transition SST turbulence model. For all turbulence models and cases, Case-2 produces the highest friction factors. This is followed by Case-4, then by Case-1 and Case-3 in the order of decreasing friction factors. The small amplitudes and frequencies produce lower friction factors.

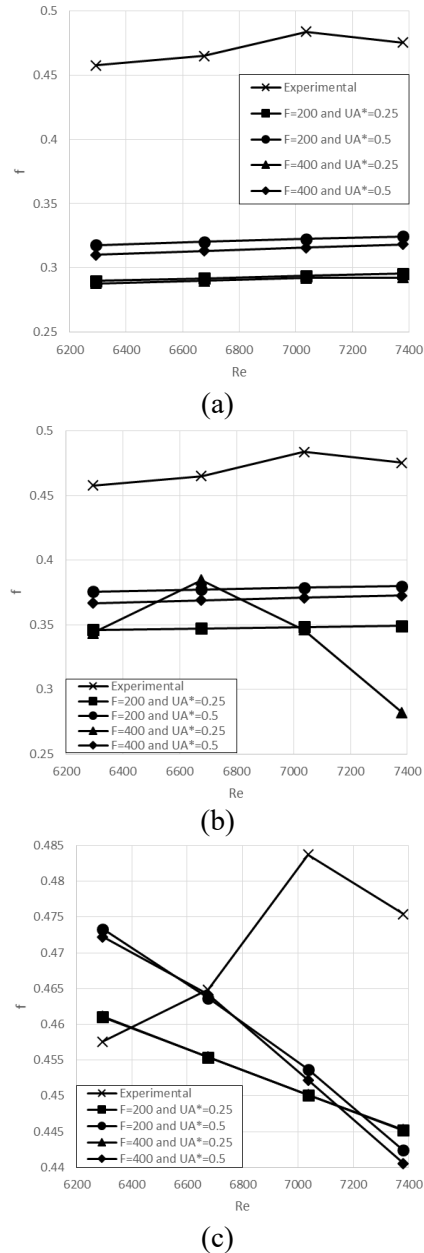


Figure 6. Changing of friction factor with Reynolds number for (a) $k-\omega$ (b) SST (c) transition SST turbulence models

As stated before, in the previous study [33], the SST turbulence model performed better than the other turbulence modes. Based on this, assuming that the SST turbulence model is accurate, we can conclude that pulsating flow is a suitable method for decreasing friction factors. The $k-\omega$ and transition SST turbulence models also estimate lower friction factors compared to the experimental, steady-state values.

5. CONCLUSIONS

The present study represents a numerical study for a wavy channel under pulsating flow conditions.

Four cases combining two different oscillation frequencies and amplitudes are used to define pulsating flow conditions. The results that is acquired from pulsatile numerical studies are compared with each other and the non-pulsating experimental results. RANS based turbulence models, which are the $k-\omega$, the SST and the transition SST models, are used. The prominent conclusions are listed as;

- Pulsating flow conditions have a positive effect to enhance heat transfer.
- With ascending Reynolds number, Nusselt number ascends
- Amplitude has a positive effect for increasing Nusselt number for all turbulence models.
- The SST and transition SST turbulence models predicts the highest Nusselt numbers, which are also higher than the non-pulsating experimental results. However the $k-\omega$ turbulence model predicts the lowest Nusselt numbers that are also lower than the non-pulsating experimental results
- Pulsating flow conditions are suitable to decrease friction factor.
- With ascending Reynolds numbers friction factors ascends for the SST and the $k-\omega$ turbulence models. Moreover, friction factor descends with ascending Reynolds number for the transitional SST turbulence model.
- For all turbulence models, the cases of small amplitudes and frequencies produce lower friction factors.
- In the future work, the new pulsating experiments has to be made for validating the numerical results

NOMENCLATURE

| | | |
|----------------------|---|--|
| D_h | : | hydraulic diameter, m |
| f | : | friction factor |
| f | : | frequency, 1/s |
| F | : | nondimensionalized frequency |
| H | : | channel height, m |
| h | : | loop average heat transfer coefficient, $W/m^2 \cdot K$ |
| h_x | : | axially local heat transfer coefficient, $W/m^2 \cdot K$ |
| k | : | thermal conductivity, $W/m \cdot K$ |
| Nu | : | Nusselt number |
| P | : | Pressure, Pa |
| Re | : | Reynolds number |
| S | : | pitch (axial length of loop), m |
| t | : | time, s |
| T | : | temperature, K |
| u | : | velocity, m/s |
| x | : | axial coordinate, m |
| Greek symbols | | |
| θ | : | contact angle, $^\circ$ |
| ρ | : | density, kg/m^3 |
| μ | : | dynamic viscosity, $kg/m \cdot s$ |
| ν | : | kinematic viscosity, m^2/s |
| Sub-and Superscripts | | |
| A | : | amplitude |
| min | : | minimum |
| max | : | maximum |
| 0 | : | uniform inlet |
| * | : | nondimensionalized |

REFERENCES

- [1] R. L. Webb, "Principles of Enhances Heat Transfer, Wiley, New York, 1994.
- [2] T. Kuppan, "Heat exchanger Design Handbook" Marcell Dekker Inc. New York, 2000.
- [3] A. C. Benim, H. Chattapadhyay, A. Nahavandi, "Computational Analysis of Turbulent Forced Convection in a Channel with a Triangular Prism", *Int. J. Thermal Sciences*, vol. 50, no.10, pp. 1973-1983, 2011.

- [4] I. Taymaz, E. Aslan, A. C. Benim, "Numerical Investigation of Incompressible Fluid Flow and Heat Transfer across a Bluff Body in a Channel Flow", *Thermal Sciences*, vol.19, no.2, pp.537-547, 2015.
- [5] S. Bhattacharyya, H. Chattopadhyay, A. C. Benim, "Simulation of Heat Transfer Enhancement in Tube Flow with Twisted Tape Insert", *Prog. Computational Fluid Dynamics*, vol. 17, no.3, pp. 193-197, 2017.
- [6] H. Chattopadhyay, A. C. Benim, "Turbulent Heat Transfer Over a Moving Surface Due to Impinging Slot Jets", *J. Heat Transfer – Tras. ASME*, vol.133, no. 10, Article Number: 104502, 5 pages, 2011.
- [7] A. C. Benim, "A Finite Element Solution of Radiative Heat Transfer in Participating Media utilizing the Moment Method", *Computer Methods Appl. Mech. Eng.*, vol. 67, no. 1, pp. 1-14, 1988.
- [8] E. M. Sparrow, L. M. Hossfeld, Effect of Rounding of Protruding Edges on Heat Transfer and Pressure Drop in a Duct" *Int. J. Heat Mass Trans.*, vol. 27, no. 10, pp. 1715-1723, 1984.
- [9] B. Snyder, K. T. Li, R. A. Wirtz, "Heat Transfer Enhancement in a Serpentine Channel", *Int. J. Heat Mass Trans.*, vol. 36, no. 12, pp. 2965-2976, 1993.
- [10] K. Bilen, M. Cetin, H. Gul, T. Balta, "The Investigation of Groove Geometry Effect on Heat Transfer for Internally Grooved Tubes", *Appl. Thermal Eng.*, vol. 29, no. 4, pp.753-761, 2009.
- [11] K. Nilpueng, S. Wongwises, "Flow Pattern and Pressure Drop of Vertical upward Gas Liquid Flow in Sinusoidal Wavy Channels", *Exp. Thermal Fluid Sci.*, vol. 15, no. 6, pp.290-306, 2006.
- [12] M. Ciofalo, J. Stasiek, M. W. Collins, "Flow and Heat Transfer in Corrugated Passages: Direct and Large Eddy Simulation and Comparison with Experimental Results" In Proc. 2nd Int. Symp. Eng. Turbulence Modelling and Measurements, Florence, Italy, pp.293-292, 1993.
- [13] M. Mirzaei, A. Sohankar, L. Davidson, F. Innings, "Large Eddy Simulation of the Flow and Heat Transfer in a Half-Corrugated Channel with Various Wave Amplitudes", *Int. J. Heat Mass Trans.*, vol. 76, pp. 432-446, 2014.
- [14] S. Ray, B. Unsal, F. Durst, "Development Length of Sinusoidally Pulsating Laminar Pipe Flows in Moderate and High Reynolds Number Regimes", *Int. J. Heat Fluid Flow*, vol. 37, pp.167-176, 2012.
- [15] C. Aygun, O. Aydin, "Hydrodynamics of Piston-Driven Laminar Pulsating Flow: Part 1. Developing Flow", *Nucl. Eng. Design*, vol. 274, pp. 164-171, 2014
- [16] C. Aygun, O. Aydin, "Hydrodynamics of Piston-Driven Laminar Pulsating Flow: Part 2. Fully Developed Flow", *Nucl. Eng. Design*, vol. 274, pp. 172-180, 2014
- [17] H. Chattopadhyay, F. Durst, S. Ray, "Analysis of Heat Transfer in Simultaneously Developing Pulsating Laminar Flow in a Pipe with Constant Wall Temperature", *Int. Com. Heat Mass Transfer*, vol. 33, no. 4, pp. 475-481, 2006.
- [18] A. C. Benim, M. Cagan, Gunes, D, "Computational Analysis of Transient Heat Transfer in Turbulent Pipe Flow", *Int. J. Thermal Sciences*, vol. 43, no. 8, pp.725-732, 2004.
- [19] D. A. Nield, A. V. Kuznetsov, "Forced Convection with Laminar Pulsating Flow in a Channel or Tube", *Int. J. Thermal Sciences*, vol. 46, pp.551-560, 2007.
- [20] C. Y. Tseng, K. S. Yang, K. H. Chien, M. Jeng, C. C. Wang, "Investigation of the Performance of Pulsating Heat Pipe Subject to Uniform/Alternating Tube Diameters", *Exp. Therm. Fluid Sciences*, vol. 54, pp.85-92, 2014.
- [21] B. Metha, S. Khandekar, "Local Experimental Heat Transfer of Single-Phase Pulsating Laminar Flow in a Square Mini-Channel", *Int. J. Thermal Sci.*, vol. 91, pp.157-166, 2015.

- [22] J. Y. Yu, W. Lin, X. T. Zheng, "Effect on the Flow and Heat Transfer Characteristics for Sinusoidal Pulsating Laminar Flow in a Heated Square Cylinder", *Heat Mass Trans.*, vol. 50, pp.849-864, 2014.
- [23] M. Jafari, M. Farhadi, K. Sedighi, "Pulsating Flow effects on Convection Heat Transfer in a Corrugated Channel: A LBM Approach", *Int. Commun. Heat Mass. Trans.*, vol. 45, pp.146-154, 2013.
- [24] F. N. van de Vosse, "Analysis of Carotid Artery Flow" Dissertation in TY Eindhoven, NL, 1987.
- [25] A. C. Benim, A. Nahavandi, A. Assmann, D. Schubert, P. Feindt, S. Suh. "Simulation of Blood Flow in Human Aorta with Emphasis on Outlet Boundary Conditions" *Appl. Math. Modelling*, vol. 35, no. 7, pp. 3175-3188, 2011.
- [26] A. Assmann, A. C. Benim, F. Gül, P. Lux, P. Akhyari, U. Boeken, F. Joos, P. Feindt, A. Lichtenberg, "Pulsatile Extracorporeal Circulation during on-pump Cardia Surgery Enhances Aortic Wall Shear Stress" , *J. Biomechanics*, vol. 45, no. 1, pp.156-163, 2012.
- [27] A. C. Benim, F. Gül, A. Assmann, P. Akhayari, A. Lichtenberg, F. Joos, "Validation of Loss-Coefficient-Based Outlet Boundary Conditions for Simulating Aortic Flow" *J. Mechanics and Medicine Biology*, vol. 16, no. 2, Article Number: 1650011, 15 pages, 2016.
- [28] Ansys-Fluent, Ansys Fluent 14.5 User's Guide, Canonsburg, PA, 2012.
- [29] D. C. Wilcox, "Turbulence Modelling for CFD", DCW Industries, Inc., La Canada, California, 1998
- [30] F. R. Menter," Two-Equation Eddy-Viscosity Turbulence Models for Engineering Applications", *AIAA Journal*, vol. 32, no. 8, pp.1598-1605, 1994.
- [31] F. R. Menter, R. Langtry, S. Volker, "Transition Modelling for General Purpose CFD Codes", *Turbulence Combustion*, vol. 77, no. 1, pp.277-303, 2006.
- [32] P. A. Durbin, B. A. P. Reif, "Statistical Theory and Modelling for Turbulent Flows" 2nd ed, Wiley Chichester, 2011.
- [33] E. Aslan, I. Taymaz, Y. Islamoglu, M. Engin, I. Colpan, G. Karabas, G. Ozcelik, "Computational Investigation of the Velocity and temperature Fields in Corrugated Heat Exchanger Channels Using RANS based Turbulence Models with Experimental Validation", *Prog. Computational Fluid Dynamics*, vol. 18, no.1, pp. 33-45, 2018.
- [34] A. C. Benim, K. Ozkan, M. Cagan, D. Gunes, "Computational Investigation of Turbulent Jet Impinging onto Rotating Disk", *Int. J. Numerical Methods Heat Fluid Flow*, vol. 17, no. 3, pp.284-301, 2007.
- [35] P. Oclon, S. Lopata, M. Nowak, A. C. Benim, "Numerical Study on the Effect Inner Tube Fuling on the Therma Performance of High-Temperature Fin-and-tube Heat Echanger" *Prog. Computational Fluid Dynamics*, vol. 15, no.5, pp. 290-306, 2015.